Supporting information for

Porous $TiNi_3$-based Intermetallics as Active and Robust Monolith Catalysts for Hydrogen Evolution

Yue Qiu, Zhenli He, Yuehui He, Qian Zhao, Zhonghe Wang, and Yao Jiang*

State Key Laboratory of Powder Metallurgy, Powder Metallurgy Research Institute, Central South University, Changsha 410083, Hunan, China.

*To whom correspondence should be addressed.

E-mail: jiangyao@csu.edu.cn.

Experimental section:

Chemicals: Ti powders (D_{50} = 28.7 μm, 99.9%), Ni powders (D_{50} = 33.1 μm,99.9%), and Mo powders (D_{50} = 9.88 μm, 99.9%) were purchased from Beijing Xingrongyuan Technology Co. Ltd (Figure S13, ESI†). Nafion solution (~5 wt% in a mixture of lower aliphatic alcohols and water) was purchased from Sigma-Aldich. The commercial Pt/C (20 wt% loading) was purchased from Johnson Matthey (JM). Isopropanol (C_3H_8O, >99.7%) was purchased from Sinopharm Chemical Reagent Co. Ltd. (Shanghai, China). The water (18 MΩ/cm) used in all experiments was prepared by passing through an ultra-pure purification system (Aqua Solution).

Synthesis of $TiNi_3$ Monolith Catalyst. First, Ti powders and Ni powders were mechanically mixed for 48 h at an atomic ratio of 1:3. Then the mixed powders were loaded into a sintering boat of size 15 × 76 × 11 mm and loose-powder sintering. The whole sintering process consisted of six stages: 120℃ holding 0.5 h, 600°C holding 10 min, 750°C holding 1.5 h, 900°C holding 2 h, 1100°C holding 2 h, and 1300°C holding 6 h. Finally, the sample cooled to room temperature, and the $TiNi_3$ porous monolith catalyst (PMC) was obtained.

Synthesis of Mo-$TiNi_3$ Monolith Catalyst. The synthesis method of Mo-$TiNi_3$ was the same as that of $TiNi_3$, except that Mo powders were used. Mo powders of different contents 2, 8, and 10 % were mixed well with Ti powders and Ni powders(denote as

Mo-$TiNi_3$-2%, Mo-$TiNi_3$-8%, and Mo-$TiNi_3$-10%, respectively), and then synthesised by the above methods.

Synthesis of $TiNi_3$/Mo(10%) physical mixture powders catalyst. $TiNi_3$ was ground to a 30 μm powders. 84.006 mg $TiNi_3$ powders and 15.996 mg Mo powders were taken and dispersed in 720 μL water, 240 μL isopropanol and 40 μL Nafion (5 wt%) solution. The mixture was then sonicated for 30 minutes to form a homogeneous ink. Finally, the catalyst ink was loaded onto the Ni Foam substrate to give a mass loading of approximately 20 mg cm^2 and dried naturally for electrochemical tests.

Synthesis of Mo-$TiNi_3$-10% doped powders catalyst. Mo-$TiNi_3$-10% was ground to a 30 μm powders, 100 mg of Mo-$TiNi_3$-10% powders were loaded onto nickel foam in the same way for electrochemical testing.

Material characterization. The phase of porous materials was measured by X-ray diffractometer (RigakuD/Max2500). The X-ray source was Cu kα (λ = 0.154056 nm). The grazing incidence XRD data are recorded by the Rigaku Smartlab instrument, and the grazing incidence angle is 0.1 °. The morphology of porous materials was analyzed by field emission scanning electron microscope (MIRA 3). X-ray photoelectron spectroscopy (ESCALABSB250 Xi) was used to analyze the valence of elements. The X-ray source was Al Kα and the scanning step was 0.05eV. The pore size distribution of porous materials is tested by the Automatic mercury porosimeter (AutoPore IV 9500). The specific surface area of porous materials is measured by the Automatic surface area and porosity analyzer (ASAP2460).

Electrochemical Measurements. The HER test was performed on a CHI660D workstation under room temperature and atmospheric pressure. A typical three-electrode system was used to conduct electrochemical measurements under alkaline condition (1 M KOH), with a working electrode, a saturated calomel electrode (SCE) as the reference electrode, and a graphite carbon rod as the counter electrode. The $TiNi_3$-based PMCs were used as the working electrode with an electrode area of 1 cm^2, and commercial Pt/C (20 wt% Pt) was used as comparison. The commercial Pt/C ink was

prepared by dissolving 2 mg commercially available Pt/C in 400 μL isopropanol along with 10 μL Nafion sonicated for 10 min. 10 μL ink was dropped on the glassy carbon electrode (GCE) for electrochemical tests. The electrode to be tested was polarized at constant current under 10 mA cm^{-2} current density for 6 h to achieve the best performance before testing. According to the relationship between the potential in the Nernst equation and the saturated calomel electrode, the saturated calomel electrode potential is transformed into a pair of reversible hydrogen electrode potential.

$$E_{RHE} = E_{SCE} + E_{REF} + 0.059pH - iR_s \quad (1)$$

Where E_{RHE} is the potential of the reversible hydrogen electrode after conversion, E_{SCE} is the measured potential, E_{REF} is the electrode potential of calomel electrode in saturated KCl solution, i is the measured current, and R_S is the uncompensated resistance.

The linear sweep voltammetry (LSV) curves were obtained at a scan rate of 1 mV s^{-1}, the iR compensation percentage was 90%. The frequency range of Electrochemical Impedance Spectroscopy (EIS) test was 10^{-2}–10^5 Hz with an amplitude of 5 mV. Cyclic voltammetry (CV) curves were carried out at different scanning rates (60, 70, 80, 90, and 100 mV s^{-1}) in the non-Faradic region. The electrochemical active surface area (ECSA) is estimated according to the double-layer capacitance.

Computational methods. Our calculations were performed by means of density functional theory (DFT) using the Vienna Ab-initio Simulation Package (VASP).[1-3] The electron-ion interactions were described by using projector augmented wave (PAW) method.[4] The cutoff energy for the plane wave-basis expansion was set to 400 eV. The convergence criterion of electronic structure was set to 10^{-4} eV, and the atomic relaxation was continued until the forces acting on atoms were smaller than 0.02 eV/Å. The Brillouin zone was sampled with 3×4×1 Monkhorst-Pack k-point mesh, and a Gaussian smearing of 0.05 eV was applied to speed up electronic convergence. The 4-layer $2\sqrt{2} \times \sqrt{2}$ supercell of $TiNi_3$ (004) was used to build the calculation models, and an additional vacuum layer of 20 Å was added to the model to avoid the artificial interaction effect between the slab and their mirror images. A surface Ti or Ni atom was replaced with Mo atom to build the Mo-$TiNi_3$ (Ti site) and Mo-$TiNi_3$ (Ni site)

models. In the structure optimization, the bottom 2-layer atoms were fixed, and the other atoms were fully relaxed. The final structure was illustrated with VESTA software.[5]

The hydrogen adsorption free energy was calculated by

$$\Delta G_H = E(*H) - E(*) - 1/2E(H_2) + 0.24 \quad (2)$$

where $E(*H)$ and $E(*)$ were the total energies of the $TiNi_3$ based PMC surface with and without hydrogen adsorption, $E(H_2)$ was the total energy of hydrogen molecule in vacauum. Besides, a empirical 0.24 eV parameter was chosen to evaluate the zero-point energy and entropy contribution as our previous work.[6]

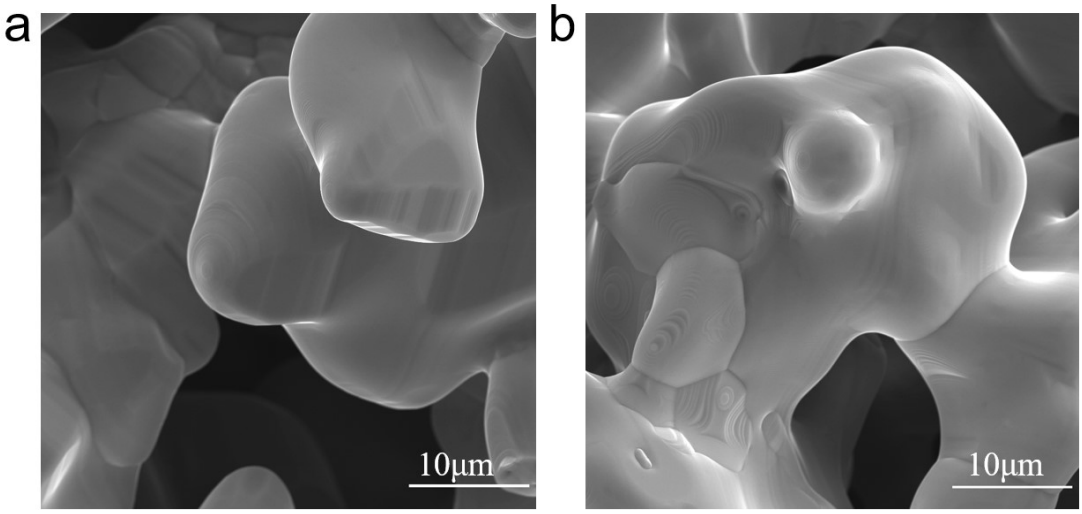

Fig. S1. SEM images. a) Mo-$TiNi_3$-2%. b) Mo-$TiNi_3$-8%.

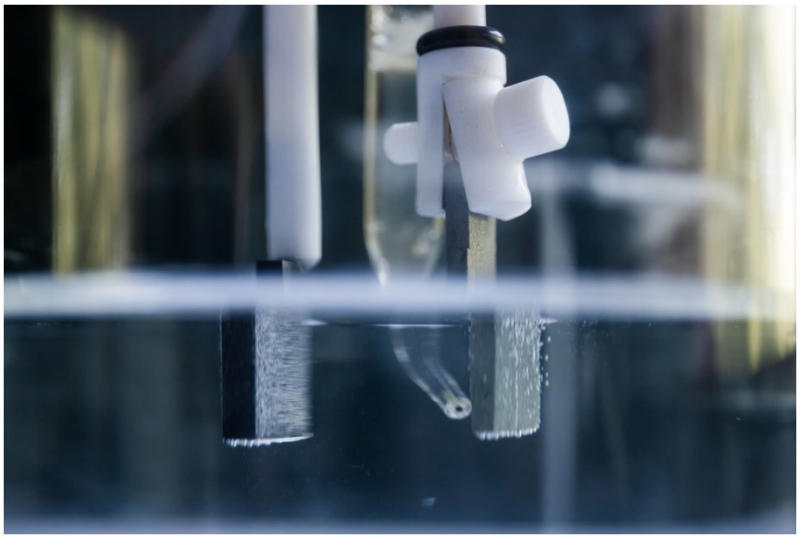

Fig. S2. Photo image of the gas bubble.

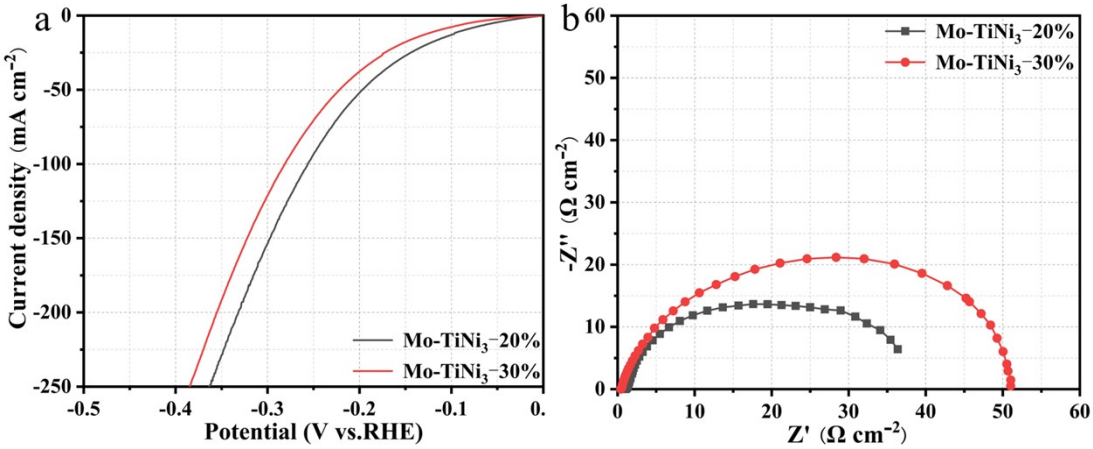

Fig. S3. HER performance of the Mo-TiNi$_3$-20% and Mo-TiNi$_3$-30%. (a) LSV curves. (b) EIS curves.

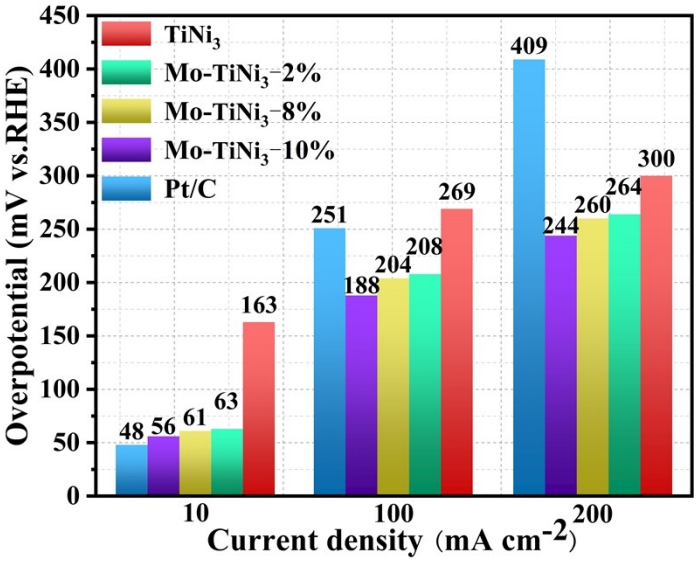

Fig. S4. The overpotential of PMCs at different current densities.

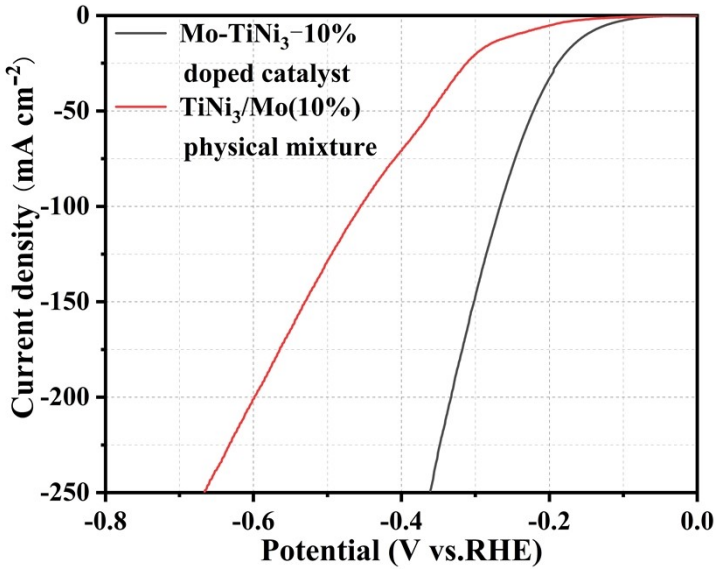

Fig. S5. LSV curves of Mo-$TiNi_3$-10% (doped catalyst) and $TiNi_3$/Mo (10%) (physical mixture) powders.

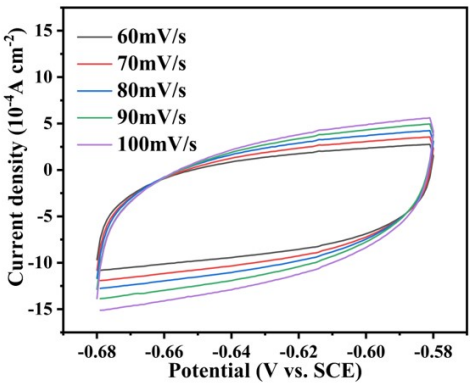

Fig. S6. CV curves of $TiNi_3$.

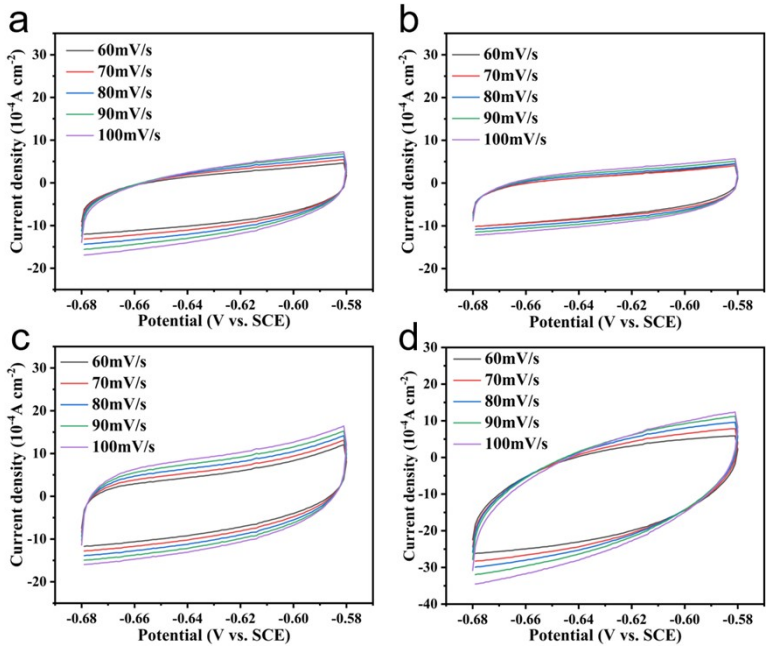

Fig. S7. CV curves. a) Mo-$TiNi_3$-2%. b) Mo-$TiNi_3$-8%. c) Mo-$TiNi_3$-10%. d) Pt/C.

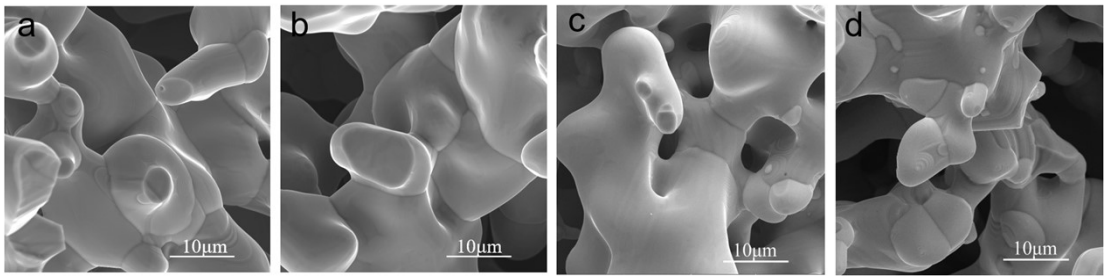

Fig. S8. SEM images of $TiNi_3$ and Mo-$TiNi_3$-10% PMC (a-b) $TiNi_3$ PMC before and after 48 h stability test. (c-d) Mo-$TiNi_3$-10% PMC before and after 48 h stability test.

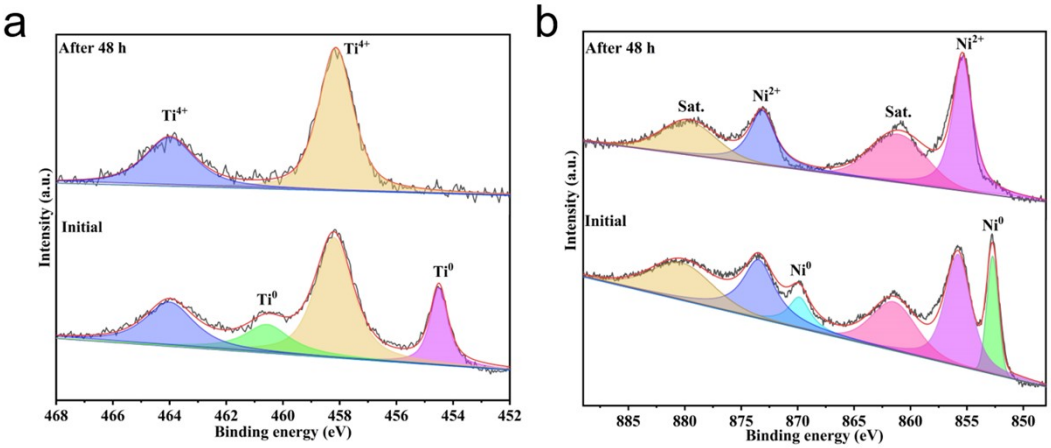

Fig. S9. XPS spectrum of $TiNi_3$. a) Ti 2p. b) Ni 2p.

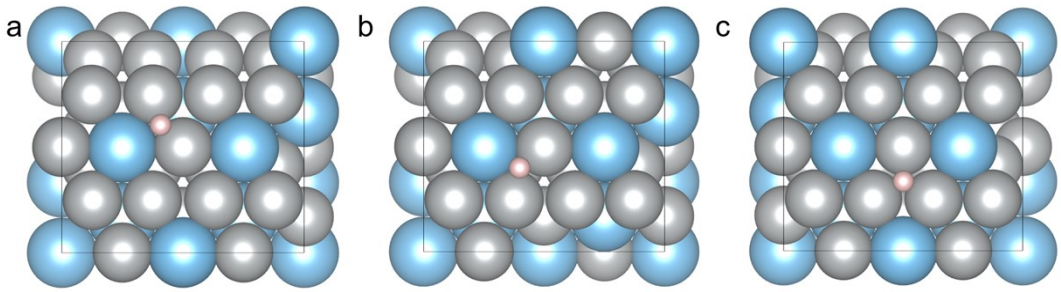

Fig. S10. Theoretical adsorption models. a) $TiNi_3$ (1 site). b) $TiNi_3$ (2 site). c) $TiNi_3$ (3 site).

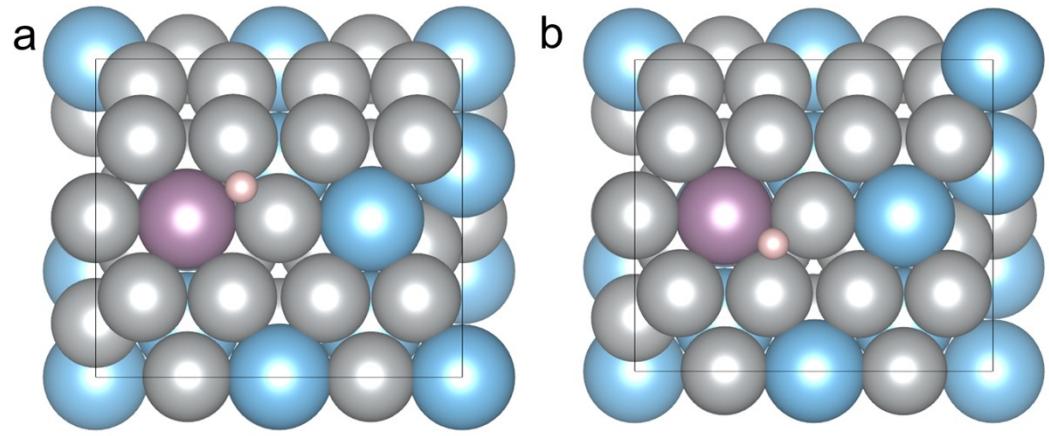

Fig. S11. Theoretical adsorption models. a) Mo-$TiNi_3$ (Ti 1 site). b) $TiNi_3$ (Ti 2 site).

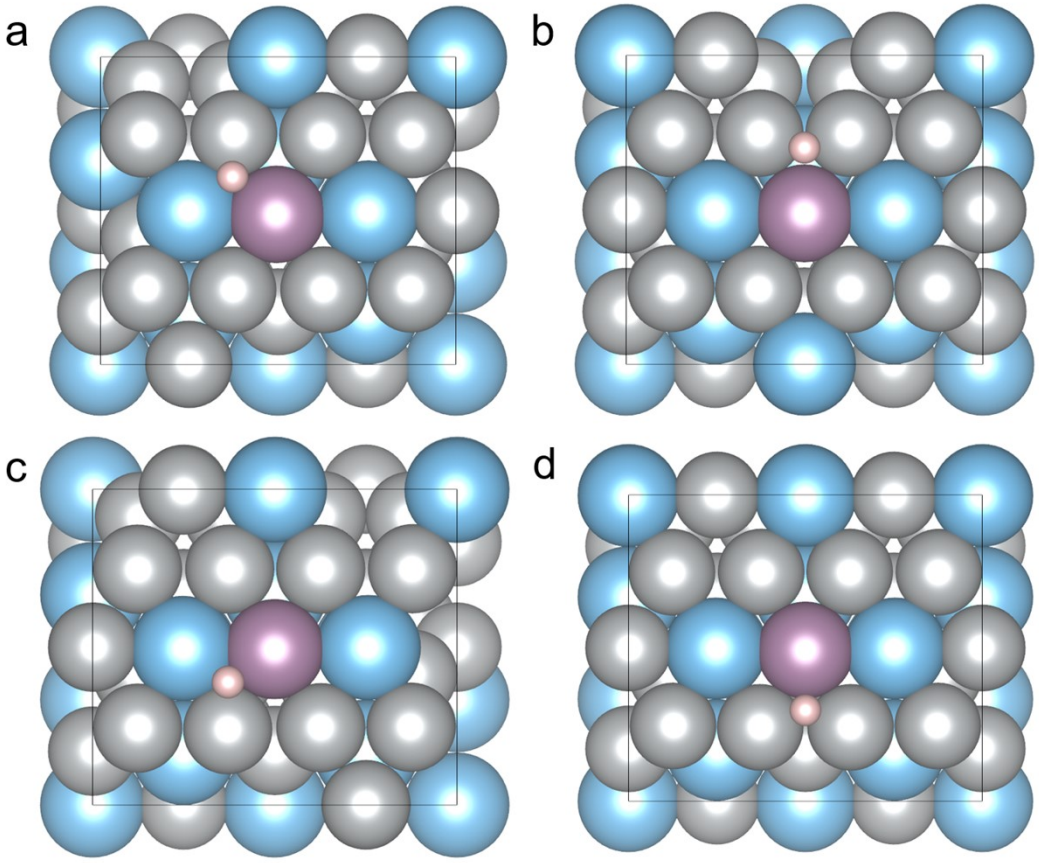

Fig. S12 Theoretical adsorption models. a) Mo-$TiNi_3$ (Ni 1 site). b) $TiNi_3$ (Ni 2 site). c) $TiNi_3$ (Ni 3 site). d) $TiNi_3$ (Ni 4 site).

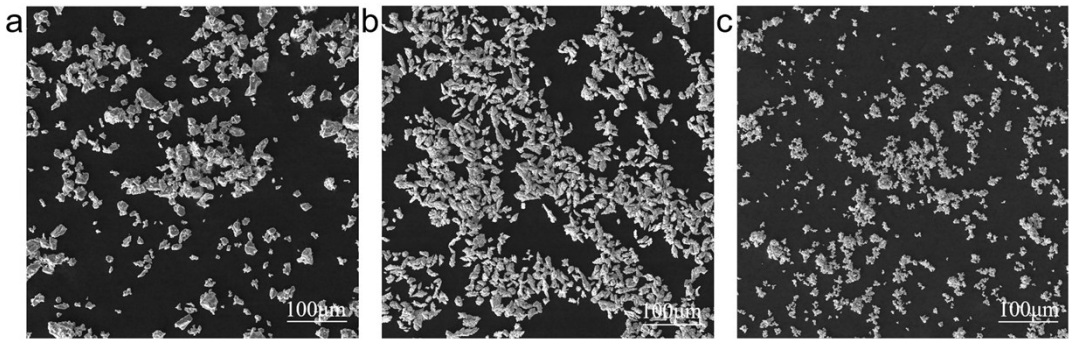

Fig. S13. SEM images of powders. a) Ti powders. b) Ni powders. c) Mo powders.

Table S1. HER activities of the reported electrocatalysts in 1 M KOH.

Electrocatalysts	Overpotential at 10 mA cm^{-2} (mV)	Tafel slope ($mV\ dec^{-1}$)	Ref.
Mo-$TiNi_3$-10%	51	56	This work
Ni_5P_4-Ru/CC	54	52	7
Ni@Ni_2PRu	43	41	8
R-NiRu	16	40	9
NiMoN	56	45.6	10
NiFeRu-LDH	29	31	11
NiVRu-LDH	12	40	12
Ni_3N@CQDs	69	104	13
CoNiP	58	57	14
CoP/NCNHP	115	66	15
$MoS_2/Co_9S_8/Ni_3S_2$/Ni	113	85	16
Ni-Ni_3C	98	88.5	17
Co-NiS_2	80	43	18
Ni-$Ni(OH)_2$	57	44.8	19
Ni-V_2O_3	61	79.7	20
Ni-MoS_2	98	103	21
Ni NP|Ni-N-C	147	114	22
WMo-NG	67	45	23
Mo_2N-Mo_2C	154	68	24
Ni_3S_2@BL MoS_2	78.1	53.4	25
Fe-$MoS_2/CoMo_2S_4$	122	90	26
Co_9S_8-MoS_2	167	81.7	27
MoS_2/Fe_5Ni_4S	122	45.1	28
MoS_2/Ni_2O_3H	84	82.3	29

Electrocatalysts	Overpotential at 10 mA cm^{-2} (mV)	Tafel slope (mV dec^{-1})	Ref.
H-MoS_2/MoP	92	59.8	30
Mo_2N-MoS_2 MCNFs	131	68.9	31
D-MoS_2/NiS_2	62	50.1	32
CoP/MoS_2	77	58	33
R-MoS_2@NF	71	100	34
Ni-MoS_2	98	60	35
Co-O-1T-MoS_2/SWNT	113	50	36
2D-MoS_2/Co(OH)	128	76	37

Table S2. HER activities of the reported electrocatalysts in 1 M KOH.

Electrocatalysts	Overpotential at 100 mA cm^{-2} (mV)	Tafel slope ($mV\ dec^{-1}$)	Ref.
MoO_3/Ni-NiO/CC	162	59	38
NiMoN/CC	~168	95	39
Ni_2P/NF	~175	76	40
Co/MoN/NF	179	77.5	41
Ni-Ni_4N	193	118.1	9
Ni_3N-VN/NF	218	37	42
Ni-Mo-N/CFC	~250	70	43
Co-Ni_3N/CC	~285	156	44
$Pt_{ads}@WC_X$	297	53	9

Table S3. Electrochemical stability tests of the reported electrocatalysts in 1 M KOH.

Electrocatalysts	Test conditions	Test time (h)	Ref.
Mo-$TiNi_3$-10%	100 mA cm^{-2}	48	This work
Ni-SA/NC	200 mv	14	45
D15h HEI	100 mA cm^{-2}	40	46
Pi–CoP	10 mA cm^{-2}	20	47
Ni-SN@C	25 mV	40	48
CoNi-inf	10 mA cm^{-2}	14	49
Co-Pd-MoS_2	49.3 mV	32	50
Ir/VC/C-100	10 mA cm^{-2}	10	51
CoMoCH@NiCoP/NF	100 mv	50	52
SnTPPCOP	147 mV	10	53
1.0Ru@Ni_3B	10 mA cm^{-2}	24	54

References

1. G. Kresse and J. Hafner, *Phys. Rev. B*, 1993, 47, 558.
2. G. Kresse and J. Furthmüller, *Phys. Rev. B*, 1996, 54, 11169.
3. G. Kresse and J. Furthmüller, *Comput. Mater. Sci.*, 1996, 6, 15-50.
4. G. Kresse and D. Joubert, *Phys. Rev. B*, 1999, 59, 1758.
5. K. Momma and F. Izumi, *J. Appl. Crystallogr.*, 2011, 44, 1272-1276.
6. Y. Ji, H. Dong, C. Liu and Y. Li, *Nanoscale*, 2019, 11, 454-458.
7. Q. He, D. Tian, H. Jiang, D. Cao, S. Wei, D. Liu, P. Song, Y. Lin and L. Song, *Adv. Mater.*, 2020, 32, 1906972.
8. Y. Liu, S. Liu, Y. Wang, Q. Zhang, L. Gu, S. Zhao, D. Xu, Y. Li, J. Bao and Z. Dai, *J. Am. Chem. Soc.*, 2018, 140, 2731-2734.
9. X. Chen, J. Wan, J. Wang, Q. Zhang, L. Gu, L. Zheng, N. Wang and R. Yu, *Adv. Mater.*, 2021, 33, 2104764.
10. L. Yu, Q. Zhu, S. Song, B. McElhenny, D. Wang, C. Wu, Z. Qin, J. Bao, Y. Yu and S. Chen, *Nat. Commun.*, 2019, 10, 1-10.
11. G. Chen, T. Wang, J. Zhang, P. Liu, H. Sun, X. Zhuang, M. Chen and X. Feng, *Adv. Mater.*, 2018, 30, 1706279.
12. D. Wang, Q. Li, C. Han, Q. Lu, Z. Xing and X. Yang, *Nat. Commun.*, 2019, 10, 3899.
13. M. Zhou, Q. Weng, Z. I. Popov, Y. Yang, L. Y. Antipina, P. B. Sorokin, X. Wang, Y. Bando and D. Golberg, *ACS nano*, 2018, 12, 4148-4155.
14. Z. Fang, L. Peng, Y. Qian, X. Zhang, Y. Xie, J. J. Cha and G. Yu, J *J. Am. Chem. Soc.*, 2018, 140, 5241-5247.
15. Y. Pan, K. Sun, S. Liu, X. Cao, K. Wu, W.-C. Cheong, Z. Chen, Y. Wang, Y. Li and Y. Liu, *J. Am. Chem. Soc.*, 2018, 140, 2610-2618.
16. Y. Yang, H. Yao, Z. Yu, S. M. Islam, H. He, M. Yuan, Y. Yue, K. Xu, W. Hao and G. Sun, *J. Am. Chem. Soc.*, 2019, 141, 10417-10430.
17. P. Wang, R. Qin, P. Ji, Z. Pu, J. Zhu, C. Lin, Y. Zhao, H. Tang, W. Li and S. Mu, *Small*, 2020, 16, 2001642.

18. J. Yin, J. Jin, H. Zhang, M. Lu, Y. Peng, B. Huang, P. Xi and C. H. Yan, *Angew. Chem. Int. Ed.*, 2019, 131, 18849-18855.

19. J. Hu, S. Li, Y. Li, J. Wang, Y. Du, Z. Li, X. Han, J. Sun and P. Xu, *J. Mater. Chem. A*, 2020, 8, 23323-23329.

20. M. Ming, Y. Ma, Y. Zhang, L.-B. Huang, L. Zhao, Y.-Y. Chen, X. Zhang, G. Fan and J.-S. Hu, *J. Mater. Chem. A*, 2018, 6, 21452-21457.

21. Q. Wang, Z. L. Zhao, S. Dong, D. He, M. J. Lawrence, S. Han, C. Cai, S. Xiang, P. Rodriguez and B. Xiang, *Nano Energy*, 2018, 53, 458-467.

22. C. Lei, Y. Wang, Y. Hou, P. Liu, J. Yang, T. Zhang, X. Zhuang, M. Chen, B. Yang and L. Lei, *Energy Environ. Sci.*, 2019, 12, 149-156.

23. Y. Yang, Y. Qian, H. Li, Z. Zhang, Y. Mu, D. Do, B. Zhou, J. Dong, W. Yan and Y. Qin, *Sci. Adv.*, 2020, 6, eaba6586.

24. H. Yan, Y. Xie, Y. Jiao, A. Wu, C. Tian, X. Zhang, L. Wang and H. Fu, *Adv. Mater.*, 2018, 30, 1704156.

25. T. Zhang, Y. Liu, J. Yu, Q. Ye, L. Yang, Y. Li and H. J. Fan, *Adv. Mater.*, 2022, 2202195.

26. Y. Guo, J. Tang, J. Henzie, B. Jiang, W. Xia, T. Chen, Y. Bando, Y.-M. Kang, M. S. A. Hossain and Y. Sugahara, *ACS nano*, 2020, 14, 4141-4152.

27. M. Kim, M. A. R. Anjum, M. Choi, H. Y. Jeong, S. H. Choi, N. Park and J. S. Lee, *Adv. Funct. Mater.*, 2020, 30, 2002536.

28. Y. Wu, F. Li, W. Chen, Q. Xiang, Y. Ma, H. Zhu, P. Tao, C. Song, W. Shang and T. Deng, *Adv. Mater.*, 2018, 30, 1803151.

29. J. Hu, C. Zhang, Y. Zhang, B. Yang, Q. Qi, M. Sun, F. Zi, M. K. Leung and B. Huang, *Small*, 2020, 16, 2002212.

30. Q. Liu, Z. Xue, B. Jia, Q. Liu, K. Liu, Y. Lin, M. Liu, Y. Li and G. Li, *Small*, 2020, 16, 2002482.

31. D. Xie, G. Yang, D. Yu, Y. Hao, S. Han, Y. Cheng, F. Hu, L. Li, H. Wei and C. Ji, *ACS Sustainable Chem. Eng.*, 2020, 8, 14179-14189.

32. J. Lin, P. Wang, H. Wang, C. Li, X. Si, J. Qi, J. Cao, Z. Zhong, W. Fei and J. Feng, *Adv. Sci.*, 2019, 6, 1900246.

33. Y. Ge, H. Chu, J. Chen, P. Zhuang, Q. Feng, W. R. Smith, P. Dong, M. Ye and J. Shen, *ACS Sustainable Chem. Eng.*, 2019, 7, 10105-10111.

34. M. A. R. Anjum, H. Y. Jeong, M. H. Lee, H. S. Shin and J. S. Lee, *Adv. Mater.*, 2018, 30, 1707105.

35. J. Zhang, T. Wang, P. Liu, S. Liu, R. Dong, X. Zhuang, M. Chen and X. Feng, *Energy Environ. Sci.*, 2016, 9, 2789-2793.

36. D. Cao, K. Ye, O. A. Moses, W. Xu, D. Liu, P. Song, C. Wu, C. Wang, S. Ding and S. Chen, *ACS nano*, 2019, 13, 11733-11740.

37. Z. Zhu, H. Yin, C. T. He, M. Al‐Mamun, P. Liu, L. Jiang, Y. Zhao, Y. Wang, H. G. Yang and Z. Tang, *Adv. Mater.*, 2018, 30, 1801171.

38. X. Xiao, X. Wang, B. Li, X. Jiang, Y. Zhang, M. Li, S. Song, S. Chen, M. Wang, Y. Shen and Z. Ren, *Mater. Today Phys*., 2020, 12, 100182.

39. Y. Zhang, B. Ouyang, J. Xu, S. Chen, R. S. Rawat and H. J. Fan, *Adv. Energy Mater*., 2016, 6, 1600221.

40. X. Yu, Z.-Y. Yu, X.-L. Zhang, Y.-R. Zheng, Y. Duan, Q. Gao, R. Wu, B. Sun, M.-R. Gao, G. Wang and S.-H. Yu, *J. Am. Chem. Soc*., 2019, 141, 7537-7543.

41. J. Sun, W. Xu, C. Lv, L. Zhang, M. Shakouri, Y. Peng, Q. Wang, X. Yang, D. Yuan, M. Huang, Y. Hu, D. Yang and L. Zhang, *Appl. Catal., B*, 2021, 286, 119882.

42. H. Yan, Y. Xie, A. Wu, Z. Cai, L. Wang, C. Tian, X. Zhang and H. Fu, *Adv. Mater*., 2019, 31, 1901174.

43. Y. Li, X. Wei, L. Chen, J. Shi and M. He, *Nat. Commun*., 2019, 10, 5335.

44. C. Zhu, A.-L. Wang, W. Xiao, D. Chao, X. Zhang, N. H. Tiep, S. Chen, J. Kang, X. Wang, J. Ding, J. Wang, H. Zhang and H. J. Fan, *Adv. Mater*., 2018, 30, 1705516.

45. W. Zang, T. Sun, T. Yang, S. Xi, M. Waqar, Z. Kou, Z. Lyu, Y. P. Feng, J. Wang and S. J. Pennycook, Advanced Materials, 2021, 33, 2003846.

46. Z. Jia, T. Yang, L. Sun, Y. Zhao, W. Li, J. Luan, F. Lyu, L. C. Zhang, J. J. Kruzic and J. J. Kai, Advanced Materials, 2020, 32, 2000385.

47. D. Zhu, L. Wang, M. Qiao and J. Liu, Chemical Communications, 2020, 56, 7159-7162.

48. H. Jin, X. Wang, C. Tang, A. Vasileff, L. Li, A. Slattery and S. Z. Qiao, Advanced Materials, 2021, 33, 2007508.

49. X. Tan, S. Geng, Y. Ji, Q. Shao, T. Zhu, P. Wang, Y. Li and X. Huang, Advanced Materials, 2020, 32, 2002857.
50. W. Yang, S. Zhang, Q. Chen, C. Zhang, Y. Wei, H. Jiang, Y. Lin, M. Zhao, Q. He and X. Wang, Advanced Materials, 2020, 32, 2001167.
51. P. Wu, J. Li, Z. Xiao, Y. Zhao, Y. Wang, B. Xiao and B. Huang, Chemical Communications, 2021, 57, 10395-10398.
52. D. Guo, H. Chen, H. Tian, S. Ouyang, J. Wang and J. Lv, Chemical Communications, 2020, 56, 4990-4993.
53. Q. Wang, A. Wang, Y. Dou, X. Shen, M. S. Sudi, L. Zhao, W. Zhu and L. Li, Chemical Communications, 2022, 58, 7423-7426.
54. J. Yao, X. Zhong, T. Lu and Y. Pan, Chemical Communications, 2022 , 58, 6741-6744.